

Investigation of the frequency impact on the MIMO indoor channel capacity

A. P. Garcia^a, L. Rubio^b, G. Llano^b and J. Reig^b

^bInstituto de Telecomunicaciones y Aplicaciones Multimedia (iTEAM)

Universidad Politécnica de Valencia

Building 8G, access D, Camino de Vera, s/n 46022, Valencia (Spain)

^aInstitute of Information Technology, Ilmenau University of Technology

Corresponding author: lrubio@dcom.upv.es

Abstract

Multiple-input multiple-output (MIMO) systems have the potential to achieve very high capacity. In real environments, the maximum capacity is limited by the correlation degree among spatial subchannels. To this day, experimental studies published have focused on MIMO channels parameters at one specific central frequency and have not been examined carefully how these parameters can change with the frequency. In this paper, we investigate how the frequency can change the MIMO channel capacity in a typical indoor environment and the effects on the multivariate characteristics of a measured MIMO matrix. This study is based on a measurement campaign performed at 2, 6 and 12 GHz, considering the influence of both line-of-sight (LOS) and non-line-of-sight (NLOS) propagation conditions.

Keywords: Indoor propagation channels, MIMO channels, MIMO capacity, MIMO measurements, spatial correlation, multivariate normality, surfaces of constant variance.

1. Introduction

Multiple-input multiple-output (MIMO) systems are wireless systems with multiple antennas at the transmitter and receiver [1]. MIMO systems can be seen as beamforming, diversity or spatial multiplexing. Beamforming and diversity are concepts related to smart antennas. Nevertheless, spatial multiplexing is a new concept that permits to improve the capacity of the wireless systems without increasing the bandwidth and the transmitted power. The spatial multiplexing concept is a very powerful technique which exploits the spatial dimension (spatial subchannels) of the radio channel by simultaneous transmissions of multiple datastreams. It has been

shown theoretically that in ideal environments the capacity of a MIMO system scales linearly with the number of transmit and receive antennas considering uncorrelated channel gains [1,2]. This is due to the decomposition of the channel into an equivalent set of spatial subchannels [2]. However, the correlation among the spatial subchannels limits the achievable capacity of MIMO systems [3].

The MIMO systems are promising candidates for deployment of many wireless networks: IEEE 802.11, HipeLAN/2, MMAC (Multimedia Mobile Access Communication Systems), UWB (Ultra-WideBand), WiMAX (Worldwide Interoperability for Microwave Access), 3 GPP High-Speed Packet Access plus (HSPA+) and Long Term Evolution (LTE) are some examples. Due to the fact that these wireless systems use different frequencies, the propagation conditions observed at the radio interface will be clearly dependent to the frequency and the environment. In this sense, it is necessary to investigate how the properties of the MIMO channel change with the frequency. Experimental studies based on measurements campaigns have investigated the capacity reduction due to the spatial subchannels correlation, but these works have been focused on MIMO channel characteristics at specific central frequencies, but in different scenarios, making the comparisons difficult.

In real environments, the radio channel plays a crucial role being necessary to study how the properties of the MIMO channel characteristics change with the frequency. In [4], Maharaj *et al.* have presented an initial study aimed to understand the effect of frequency scaling on the performance of MIMO wireless systems at 2.4 and 5.2 GHz in an indoor scenario, suggesting that multipath properties are very similar in that particular environment. In this sense, and carrying on with previous author's investigations of how

the frequency can impact the MIMO channel properties [5,6], this paper presents an experimental capacity analysis for indoor MIMO systems. This analysis is based on measurements at 2, 6 and 12 GHz in an office environment, considering the spatial channel correlation effects and taking into account the same electrical separation among antenna elements. The influence of line-of-sight (LOS) and non-line-of-sight (NLOS) propagation conditions on the MIMO system capacity in terms of the frequency is also analyzed. Besides, an introduction about the frequency impact on the multivariate characteristics of a measured wideband MIMO channel is presented. As a conclusion, we have observed an ergodic and outage MIMO capacity reduction when the frequency increases, for a constant electrical separation between the transmitter and the receiver, as a consequence of the increment on the correlation degree among the spatial subchannels. From the multivariate statistical point of view, we have found remarkable differences in the multivariate normality of MIMO data at different central frequencies and array sizes.

The rest of the paper is organized as follows: Section 2 reviews the capacity of MIMO wireless channels in both theoretical and experimental ways. Section 3 describes the measurement of the MIMO radio channel. Results and discussions are given in Section 4. The conclusions are presented in Section 5.

2. Capacity of MIMO wireless channels

2.1. Theoretical capacity

Consider a MIMO system with M transmit antennas and N receive antennas. The total transmitted power is P , thereby the transmitted power by each antenna is P/M . The noise at each receiver antenna is assumed to be Gaussian, with zero mean and variance σ^2 . Let be \mathbf{H} the MIMO channel transfer matrix, with dimensions $N \times M$, and considering a flat-fading channel case. If the channel is unknown by the transmitter and perfectly known by the receiver, and waterfilling is not considered [7], the transmitted signal vector is composed of M statistically independent equal power components, each with a circularly symmetric complex Gaussian distribution, and then the channel capacity is given by [1,7]

$$C = \log_2 \left[\det \left(\mathbf{I} + \frac{P}{M\sigma^2} \mathbf{H}^H \mathbf{H} \right) \right], \quad [1]$$

where \mathbf{H}^H is the Hermitian (complex conjugate transpose) of the MIMO channel transfer matrix \mathbf{H} , \mathbf{I} is the $M \times M$ identity matrix, and $\det(\mathbf{X})$ represents the determinant of the \mathbf{X} matrix. In our analysis we have considered $M \geq N$.

The h_{ij} element of the MIMO channel transfer

matrix, \mathbf{H} , is the complex gain transmission coefficient from the j -th transmit antenna to the i -th receive antenna.

From the eigenvalues decomposition (EVD) of the $\mathbf{H}^H \mathbf{H}$, the channel capacity given by (1) is reduced to

$$C = \sum_{i=1}^k \log_2 \left(1 + \lambda_i \frac{P}{M\sigma^2} \right), \quad [2]$$

where λ_i represents the i -th eigenvalue, and $k = \text{Rank}(\mathbf{H}^H \mathbf{H}) \leq \min(M, N)$. $\text{Rank}(\cdot)$ and $\min(\cdot)$ are the rank of the matrix and the minimum value of the arguments, respectively. The i -th eigenvalue can be interpreted as the power gain of the i -th spatial subchannel [2].

In fading channels, the capacity has a random nature modelled by a random variable related to the local area or instantaneous channel realizations. To determine the cumulative distribution function (CDF) of the capacity and thereby the outage capacity, it is necessary to carry out a large number of measurements with slightly displaced arrays and considering temporally varying scatterers arrangement [8]. Since each single measurement requires an enormous effort, this procedure is highly undesirable to derive the ergodic and the outage capacities distribution. To improve this situation, in Section 3 we propose to measure the spatial correlation coefficient between two arbitrary complex gain transmission coefficients. In other words, we propose to measure the full spatial correlation matrix of the MIMO radio channel, denoted by \mathbf{R}_{MIMO} . This procedure relies on the fact that it is possible by simulation to generate different realizations of the MIMO channel transfer matrix, denoted by $\tilde{\mathbf{H}}$, from the measured \mathbf{R}_{MIMO} matrix. This procedure is explained in the next section.

2.2 Experimental capacity

From the MIMO channel transfer matrix, \mathbf{H} , the full spatial correlation matrix of the MIMO radio channel, \mathbf{R}_{MIMO} , is defined as:

where

$$\mathbf{R}_{\text{MIMO}} \triangleq E[\text{vec}(\mathbf{H})\text{vec}(\mathbf{H})^H]$$

$$\text{vec}(\mathbf{H}) \triangleq (\mathbf{h}_1^T, \mathbf{h}_2^T, \dots, \mathbf{h}_M^T)^T,$$

with

$$\mathbf{h}_j \triangleq (h_{1j}, h_{2j}, \dots, h_{Nj})^T, \quad [3]$$

$E[\cdot]$ is the expectation operator and the superscript T indicates transpose. The elements of the vector \mathbf{h}_j , h_{ij} , are the entries of the MIMO channel transfer matrix.

MIMO techniques can improve the capacity of wireless systems without increasing the bandwidth and the transmitted power

Note that \mathbf{R}_{MIMO} is a squared matrix with dimensions $MN \times MN$. From (3), the entries of the \mathbf{R}_{MIMO} matrix, ρ_{ij}^{pq} , are the correlation coefficients between couples of the transmission coefficients h_{ij} and h_{pq} , where the indexes $i-p$ refer to the receiver elements and $j-q$ to the transmitter elements:

$$\rho_{ij}^{pq} \triangleq \frac{E[h_{ij}h_{pq}^*] - E[h_{ij}]E[h_{pq}^*]}{\sqrt{E[|h_{ij}|^2] - E[h_{ij}]^2} \sqrt{E[|h_{pq}|^2] - E[h_{pq}]^2}} \quad [4]$$

To overcome the problem of the huge effort mentioned in the previous section to derive the ergodic and outage capacity experimentally, we propose to measure the correlation coefficients of the \mathbf{R}_{MIMO} matrix and then obtain by Cholesky factorization, $\mathbf{R}_{\text{MIMO}} = \mathbf{C}\mathbf{C}^T$, an observable of the MIMO channel transfer matrix, denoted by $\bar{\mathbf{H}}$, as it is explained as follows.

For simplicity, in the literature it is assumed that all the MIMO channel transfer matrices elements are complex Gaussian distributed with identical average power [9]. This assumption was checked by the authors in LOS and NLOS indoor conditions, although the approach was more realistic in NLOS conditions (the KS test was used). Then, the complex gain transmission coefficients \tilde{h}_{ij} can be generated from zero-mean complex independent identically distributed random variables, α_{ij} , as the following

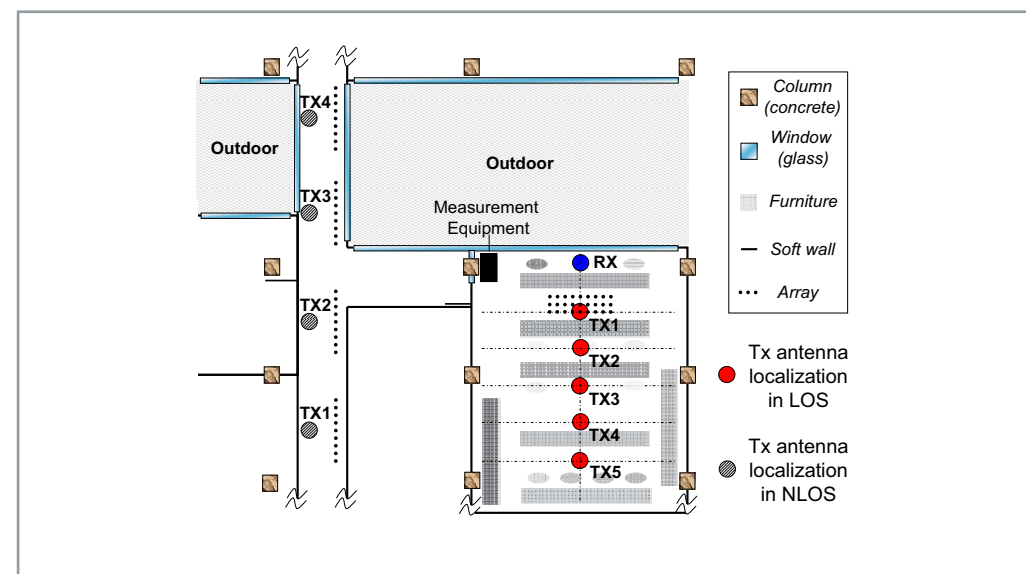
$$\mathbf{A} = \mathbf{C}\mathbf{a}, \quad [5]$$

$$\mathbf{a}_{NM \times 1} = (\tilde{h}_{11}, \tilde{h}_{21}, \dots, \tilde{h}_{N1}, \tilde{h}_{12}, \tilde{h}_{22}, \dots, \tilde{h}_{NM}, \tilde{h}_{2M}, \dots, \tilde{h}_{NM})^T$$

where

and

$$\mathbf{a}_{NM \times 1} = (\alpha_1, \alpha_2, \dots, \alpha_{NM})^T$$



■ Figure 1. Top view of the measurement environment.

Taking into account that $\text{vec}(\bar{\mathbf{H}}) \equiv \mathbf{A}$, this procedure permits us to generate observables to the MIMO channel transfer matrix, $\bar{\mathbf{H}}$, from the \mathbf{R}_{MIMO} matrix whose entries have been measured without certain difficulty. Thus, we are able to analyse the ergodic and the outage capacity. Substituting the \mathbf{H} matrix in (1) by the $\bar{\mathbf{H}}$ matrix, the capacity is derived for any $M \times N$ MIMO system configuration.

3. Measurement of the MIMO channel

This section describes the measurement location, the measuring equipment and the measuring process to collect the data required to do an experimental investigation of the MIMO channel capacity.

3.1. Measurement location

The MIMO channel measurements were carried out at the iTEAM Research Institute of the Technical University of Valencia. Fig.1 shows the top view of the measuring scenario. The outside walls of the building are formed by glass, whereas the inside walls are made of wood and wall-board. The ceilings and the floors are made of reinforced concrete over steel plates. The measurements were taken on the first floor of the building. The receiver array (RX) was placed in the office room of the Radio and Wireless Communications Group. The transmitter array (TX) was placed in the same office as the RX, where the propagation was in LOS condition, and in the adjacent corridor, where the propagation was in NLOS condition. The TX and RX positions are depicted in Fig.1. The maximum distance from the TX to the RX was 12 m. For convenience, the TX was moved instead of the RX.

3.2. Measuring equipment

The MIMO channel has been measured in the frequency domain using a vector network ana-

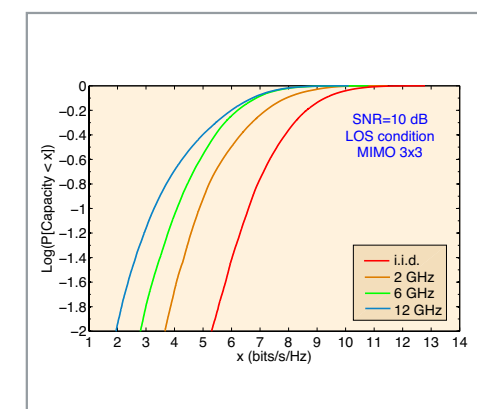
lyzer (VNA) as a channel sounder, the ZVA of Rohde & Schwarz with a dynamic range of 130 dB up to 20 GHz. Omnidirectional wideband antennas (up to 18 GHz) with flat frequency response, a wideband low noise RF amplifier at the RX, and very low attenuation cables were also used.

The antennas were set up over a precise linear positioning robotic system emulating a virtual uniform linear array (ULA) without coupling effects. We have considered a maximum number of three antenna elements at the TX and the RX in agreement with present recommendations and standards for the development of MIMO technologies [10]. The measurement process was controlled by a laptop connected to the VNA via LAN (Ethernet).

3.3. Measuring process

The transfer function in frequency domain of the radio channel, $h_{ij}(f)$, was measured between the j -th transmit and the i -receive antenna using the VNA at 2, 6 and 12 GHz central frequencies [6]. The separation among array elements was chosen in order to maintain the same electrical separation at each central frequency. To measure relative effects versus frequency, all band frequencies data were collected consecutively at the same array element positions. The H_{ij} function was measured over a bandwidth of 200 MHz (SPAN in the VNA) around each central frequency, with a frequency bin sample resolution of 50 kHz (4000 spectrum samples). At each spatial position, 50 frequency transfer function snapshots were measured and recorded (with about 120 ms. between snapshots). Then, the posterior average allowed to reduce the noise effect. The measurements were carried out at nights, in absence of people, guaranteeing stationary channel conditions.

The 200 MHz total bandwidth of the measured transfer function, $H_{ij}(f)$, was divided into 40 windows of 5 MHz, referred to $\hat{H}_{ij}(f)$, guaranteeing flat-fading channel condition (for this scenario, a coherent bandwidth around 20 MHz was checked by the authors at the 95% of locations). For each 5 MHz window, the partial spatial cor-



■ Figure 2. CDF of the 3x3 MIMO channel ergodic capacity at 2, 6 and 12 GHz in LOS conditions and with one wavelength separation among antenna elements.

relation coefficients between the transfer functions $\hat{H}_{ij}(f)$ and $\hat{H}_{pq}(f)$ were derived. Then, each spatial correlation coefficient was obtained averaging 40 partial spatial correlation coefficients.

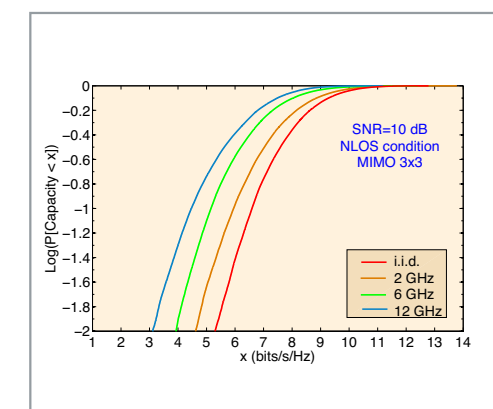
Finally, the spatial correlation coefficients defines the entries of the full spatial correlation matrix of the MIMO radio channel, \mathbf{R}_{MIMO} , at each central frequency, from which the realizations of the MIMO channel transfer matrix, $\bar{\mathbf{H}}$, are generated by the procedure described in Section 3. A total of 10^5 realizations of the $\bar{\mathbf{H}}$ matrix were considered for the results presented in the next section.

4. Results and discussions

4.1. Capacity, eigenvalues and spatial correlation

The results derived from the measurements show that the ergodic and the outage capacities decrease when the frequency increases considering the same electrical separation between antenna elements. This behaviour of the capacity with the frequency has been observed for every propagation condition, LOS and NLOS, and also for every configuration of the MIMO system in terms of the number of antennas at the TX and at the RX, $M \times N$ configuration.

Figure 2 shows the CDF of the capacity for a 3×3 MIMO configuration, with one wavelength separation among antenna elements and for SNR of 10 dB, at 2, 6 and 12 GHz in LOS conditions. As it can be seen, the capacity is reduced when the frequency increases. This behaviour also happens in NLOS conditions as it is suggested in Figure 3 for the same configuration of the MIMO system. Nevertheless, the capacity reduction is less in NLOS condition. As a measure of comparison, we have also plotted the CDF of the capacity when all the entries of the channel transfer matrix are independent and identically distributed (i.i.d.) complex Gaussian random variables. The capacity reduction observed in the real environment with respect to an i.i.d. MIMO channel is a consequence of a spatial correlation increment



■ Figure 3. CDF of the 3x3 MIMO channel ergodic capacity at 2, 6 and 12 GHz in NLOS conditions and with one wavelength separation among antenna elements.

There is a clear frequency dependence in the capacity when the electrical separation among the array elements is constant.

among the different spatial subchannels limiting the achievable capacity of the MIMO system. For a 10% of the CDF capacity, the spatial correlation among the spatial subchannels produces a reduction of about 1.7 bits/s/Hz at 2 GHz, 2.5 bits/s/Hz at 6 GHz and 3 bits/s/Hz at 12 GHz in LOS conditions. In NLOS conditions, the reduction is about 0.7 bits/s/Hz at 2 GHz, 1.5 bits/s/Hz at 6 GHz and 2 bits/s/Hz at 12 GHz. Therefore, there is a clear frequency dependence in the capacity when the electrical separation among the array elements is constant.

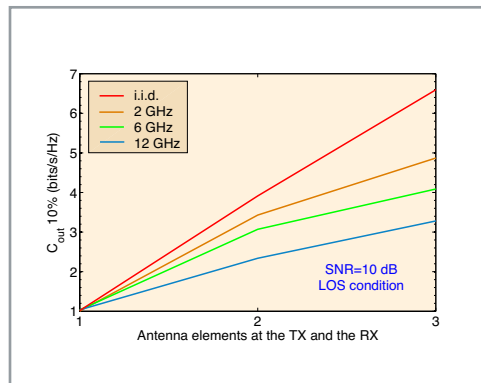


Figure 4. 10% outage capacity of the MIMO channel with one wavelength separation among antenna elements ($M=N$) at 2, 6 and 12 GHz in LOS conditions.

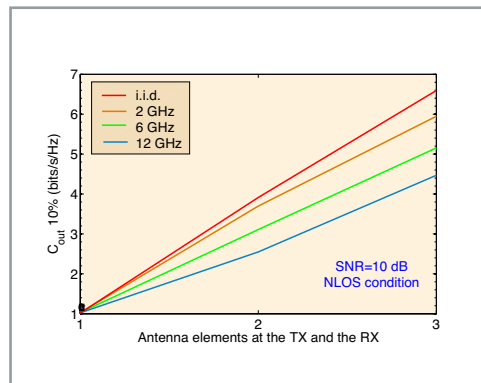


Figure 5. 10% outage capacity of the MIMO channel with one wavelength separation among antenna elements ($M=N$) at 2, 6 and 12 GHz in NLOS conditions.

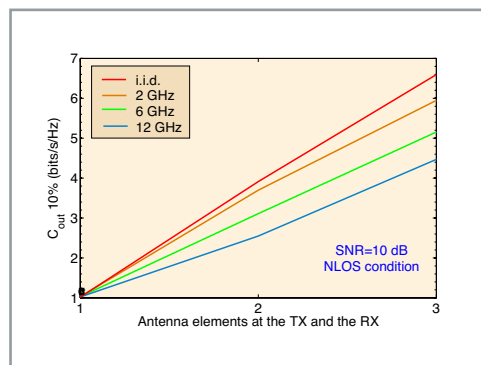


Figure 6. 11% outage capacity for a 3x3 MIMO system configuration with one wavelength separation among antenna elements versus frequency in LOS and NLOS conditions.

Figures 4 and 5 show the 10% outage capacity obtained in LOS and NLOS conditions, respectively, for a $M \times N$ ($M=N$) MIMO system configuration. A similar behaviour to the ergodic capacity is observed. Thereby, for 2×2 and 3×3 MIMO systems there is a reduction close to 1.5 bits/s/Hz from 2 GHz to 12 GHz in LOS and NLOS conditions. For the 3×3 MIMO system there is a reduction close to 3 bits/s/Hz at 12 GHz in LOS condition respect to the i.i.d. MIMO channel, whereas this reduction is about 2 bits/s/Hz in NLOS condition at the same frequency.

Figure 6 shows a comparison of the 1% outage capacity in terms of the frequency for both LOS and NLOS conditions. A 3×3 MIMO system with a SNR of 10 dB was considered. A linear trend reduction of the outage capacity with the frequency is observed. The difference between the 1% outage capacity in LOS and NLOS is about 1 bits/s/Hz at each central frequency.

The capacity reduction observed is a consequence of a volumetric increment of the environment in terms of wavelength when the frequency increases and possible changes in scatterer interactions resolution. These effects contribute to change the correlation degree among the spatial subchannels. This effect is observed in the spatial correlation values at the receiver shown in Table 1 for LOS and NLOS conditions, respectively, where the d parameter indicates the physical separation between array elements at the transmitter and the receiver sides. The correlation values that appear in bold correspond to one wavelength separation among antenna elements for each central frequency. The spatial correlation degree is equal to 0.326 and 0.283 in LOS and NLOS, respectively, at 2 GHz. These values increase up to 0.979 and 0.870 at 12 GHz in LOS and NLOS, respectively. Note that these values correspond to a maximum separation among antennas elements equal to one wavelength. These increments in the spatial correlation suggest a major spatial array elements separation when the frequency increases in order to maintain the same capacity level.

Finally, the effect of the frequency over the $\bar{\mathbf{H}}^H \bar{\mathbf{H}}$ eigenvalues matrix is shown in Figures 7 and 8, where LOS and NLOS conditions were considered, respectively. When the frequency increases, the eigenvalues reduction power gain decreases resulting in a decrement of the ergodic and outage capacities. This reduction is less in the higher eigenvalue, λ_1 . This behaviour happens in LOS and NLOS conditions, but in less proportion in NLOS. When the frequency increases, the difference in the eigenvalues power gains at 50%, 10% and 1% of the CDF suggests new considerations if the waterfilling technique is applied. At 12 GHz in LOS conditions, the power gain reduction for the smallest eigenvalues, λ_3 and λ_2 , at 1% of the CDF with respect to the i.i.d. case is about 11.5 and 10 dB, respectively, whereas the reduction for the higher eigenvalue, λ_1 , is about

d (cm.)	LOS			NLOS		
	2 GHz	6 GHz	12 GHz	2 GHz	6 GHz	12 GHz
2.5	0.945	0.921	0.979	0.820	0.924	0.870
5	0.797	0.785	---	0.579	0.780	---
7.5	0.395	---	---	0.573	---	---
10	0.387	---	---	0.275	---	---
12.5	0.331	---	---	0.262	---	---
15	0.326	---	---	0.283	---	---

Table 1. Spatial correlation coefficients at the receiver in LOS and NLOS conditions

7.5 dB. At 12 GHz in NLOS conditions the reduction is about 7.5, 6.5 and 3 dB for the eigenvalues λ_3 , λ_2 and λ_1 , respectively. Note that an increment or decrement in the frequency can modify the distribution of the eigenvalues power gains, but around the 50% the higher eigenvalue remain mostly constant.

4.2. Multivariate characteristics

Perhaps, the main assumption for the application of many covariance estimators (as needed in (3)) is the multivariate normality of MIMO data, which can be a good approximation in some cases when multivariate observations are used. From the central limit theorem, sampling distributions of certain statistics can be approximated by normal distributions, even if the data is not multivariate normal, but such approximations must be verified to apply the procedures proposed for experimental analysis of MIMO channels [11], as the techniques applied in previous sections.

For multivariate-complex-normal-distribution (MCND) analysis, in Figure 9 it is presented the 2-dimensional ellipsoids, i.e., the surfaces-of-constant-variance (SCV) for the real part of the measured multivariate vector channel $\text{vec}(\mathbf{H})$ obtained with different window widths, B , in frequency as specified in [11]. Thus, Figure 9 shows a normality visual test based on the MIMO data presented in this paper. Note that for visual MCND test, the samples of $\text{Re}\{\text{vec}(\mathbf{H})\}$ are also plotted, where $\text{Re}\{\cdot\}$ indicates real component. The configurations used for Figure 9 were as follows: $N=2$, $M=1$, $f_c=12$ GHz, and $B=\{2.5, 5, 10, 100\}$ MHz, in NLOS. These plots, based on different segmentation of data (different window widths in the frequency domain), permit a simple 2D visual test of the MCND of a measured $\text{vec}(\mathbf{H})$ for each frequency case. The conclusion is that $B=\{2.5, 5\}$ have the better fit to MCND (Figures 9.a/9.b), and the worst case is obtained for $B=100$ MHz (Figure 9.d). This conclusion is reached due to the samples are better distributed inside of the SCV for $B=\{2.5, 5\}$ than for $B=\{10, 100\}$ MHz. Note that axes h_{11} and h_{12} indicate the projected entries of the vector $\text{vec}(\mathbf{H})$ for $N=2$, $M=1$. Similar results were visualized for the imaginary part. Therefore, based on both these results and on a reliable test, e.g., multivariate Kurtosis and Skewness [11], it has been verified that $B=5$ MHz

was the best choice for channel analysis under MCND and fulfilling non-frequency selectivity in this scenario. Besides, this window selection guarantee enough number of samples for covariance estimations up to 4×4 as it was addresses in [6] and [11]. Note that this window selection was applied for the results presented in this paper.

5. Conclusions

The ergodic and the outage capacity have been investigated for a real indoor MIMO channel at 2, 6 and 12 GHz, in both LOS and NLOS conditions. The results have shown a reduction of the MIMO channel capacity when the frequency increases due to an increment of the correlation degree among the spatial subchannels. This correlation increment also produces an eigenvalues power gain reduction. Nevertheless, this reduction is less in NLOS conditions. The results are interesting for the deployment of indoor MIMO systems working at different frequencies or frequency bands close to the central frequencies considered in this study.

A procedure to obtain an experimental characterization of the MIMO channel capacity has also been presented in this paper. This procedure proposes to measure the full spatial correlation matrix of the MIMO radio channel, \mathbf{R}_{MIMO} , instead of the MIMO channel transfer matrix, \mathbf{H} , reducing the huge effort in the measurements of the channel to derive the ergodic and the outage capacities distributions.

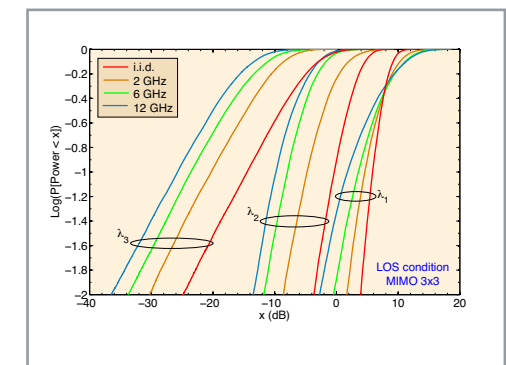
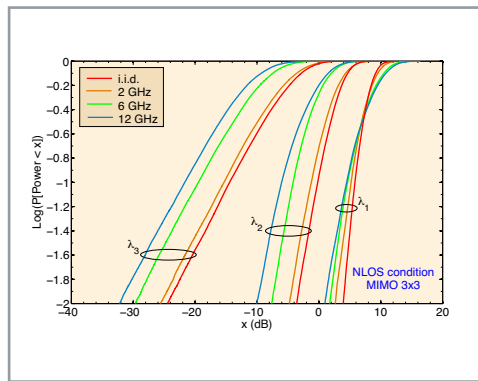
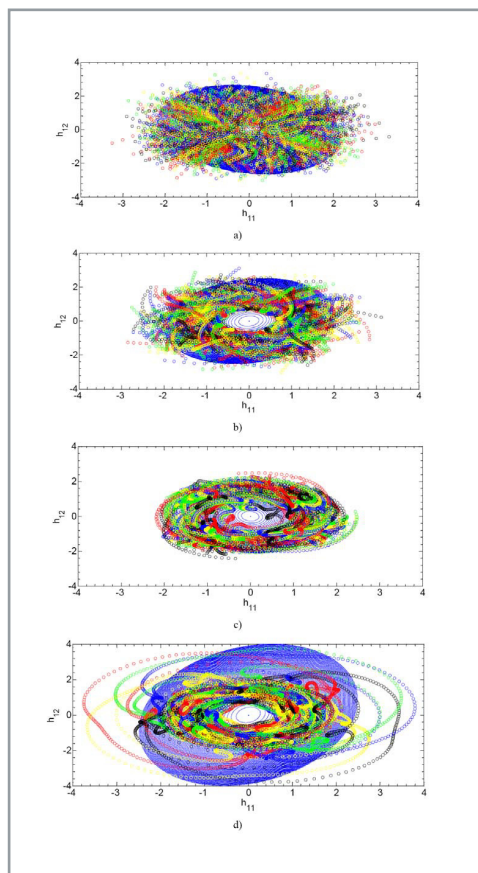


Figure 7. CDF of the eigenvalues power gain for a 3x3 MIMO system configuration with one wavelength separation among antenna elements at 2, 6 and 12 GHz in LOS conditions ($\lambda_1 > \lambda_2 > \lambda_3$).



■ **Figure 8.** CDF of the eigenvalues power gain for a 3x3 MIMO system configuration with one wavelength separation among antenna elements at 2, 6 and 12 GHz in NLOS conditions ($\lambda_1 > \lambda_2 > \lambda_3$).

For reliable estimations of \mathbf{R}_{MIMO} it was addressed the multivariate characteristics of MIMO data. The loss of normality on the observed MIMO matrix has been verified when the bandwidth was increased. Based on visual and analytical tests of MCND it was obtained the most reliable frequency segmentation for covariance estimations and channel analysis fulfilling a non-frequency selective channel.



■ **Figure 9.** Surfaces of constant variance (SCV) to test the MCND of MIMO data (real part): theoretical and experimental results for $N=2$, $M=1$, $f_c=12$ GHz in NLOS, with a) $B=2.5$ MHz, b) $B=5$ MHz, c) $B=10$ MHz, and d) $B=100$ MHz.

Hence, the objective of this paper was to analyze how the frequency could affect the capacity in a real environment considering the same electrical separation among antennas elements and the wideband effects on the multivariate distribution on MIMO data. Evidently, to have a complete understanding of the frequency impact on the MIMO channel characteristics, e.g., its ergodic capacity, the maximum achievable capacities and the MCND of experimental MIMO data, more measurements are necessary in many different indoor environments at different central frequencies and bandwidths.

References

- [1] G. J. Foschini and M. J. Gans, "On limits of wireless communications in a fading environment when using multiple antennas," *Wireless Pers. Commun.*, vol. 6, pp. 311-335, 1998.
- [2] J. B. Andersen, "Array gain and capacity for known random channels with multiple elements arrays at both ends," *IEEE J. Select. Areas Commun.*, vol. 18, pp. 2172-2178, 2000.
- [3] D. S. Shiu, G. J. Foschini, M. J. Gans, and J. M. Kahn, "Fading correlation and its effect on the capacity of multi-element antenna systems," *IEEE Trans. Commun.*, vol. 48, pp. 502-513, 2000.
- [4] B. T. Maharaj, J. W. Wallace, L. P. Linde and M. A. Jensen, "Frequency scaling of spatial correlation from co-located 2.4 and 5.2 GHz wideband indoor MIMO channel measurements," *IEE Elec. Letters*, vol. 41, No. 6, 2005.
- [5] A. P. García, L. Rubio, J. A. Díaz and N. Cardona, "Eigen/capacity analysis for indoor correlated MIMO channels between 2 and 4 GHz," *IEEE International Symposium on Wireless Communications System*, 2006.
- [6] A. P. García and L. Rubio, "Frequency dependent indoor MIMO channel characterisation between 2 and 12 GHz based on full spatial correlation matrices," *Journal of Communications*, Academy Publisher, Vo. 3, No. 4, pp. 8-15, 2008.
- [7] A. Paulraj, R. Nabar and D. Gore, *Introduction to space-time wireless communications*, Cambridge University Press, UK, 2003.
- [8] A. F. Molisch, M. Steinbauer, M. Toeltsch, E. Bonei and R. S. Thomä, "Capacity of MIMO systems based on measured wireless channels," *IEEE J. Select. Areas Commun.*, Vol. 20, No. 3, pp. 561-569, 2002.
- [9] J. P. Kermaol, L. Schumacher, K. I. Pedersen, P. E. Mogensen and F. Frederiksen, "A stochastic MIMO radio channel model with experimental validation," *IEEE J. Select. Areas Commun.*, Vol. 20, No. 6, 2002.
- [10] "Multiple-Input Multiple Output in UTRA", 3GPP TR 25.876 V1.8.0., 15th Dec. 2005.
- [11] A.P. Garcia, "PhD Dissertation: Modelling and experimental analysis of frequency dependent MIMO channels," Universidad Politécnica de Valencia - UPV, Valencia, Spain, 2009. Available in: dSPACE.upv.es/xmlui/bitstream/handle/10251/6563/tesisUPV3172.pdf?sequence=1

Bibliographies



Alexis Paolo García Ariza

was born in Bucaramanga, Colombia. He received his M.S. degree in Electronic Engineering from the Industrial University of Santander (UIS), Bucaramanga, Colombia, in

2002, and the Ph.D. degree in Telecommunications Engineering from the Technical University of Valencia, Spain, in 2009. He was with RadioGIS research group at UIS between 2002 and 2004. He was also a Research Engineer at the iTEAM Research Institute at UPV between 2004 and 2008. He is currently a Research Assistant at the Electronic Measurement Research Lab, Institute of Information Technology, Ilmenau University of Technology, Ilmenau, Germany. His research is focused on modelling, simulation and measurement/sounding of wireless channels, with special interest in wideband MIMO channels, ultra-wideband (UWB) channels, millimetre-wave (mm-Wave) channels, and time-varying shadowing. Currently he is involved in developing 60 GHz-UWB dual-polarized frontends and architectures for real-time channel sounding applied to multi Giga-bit/s access. Other areas of his interest are propagation modelling applied to Andean conditions and satellite links, and radio network planning for cellular and DVB-H/SH systems based on Geographic Information Systems (GIS).



Lorenzo Rubio

received the Telecommunication Engineering and the Ph.D degrees from the Universidad Politécnica de Valencia (UPV), Spain, in 1996 and 2004 respectively. In 1996, he joined the Communications Department of the UPV, where he is now Associate Professor of wireless communications. He is a member of the Radio and Wireless Communications Group (RWCG) of the Telecommunications and Multimedia Applications Research Institute (iTEAM). His main research interests are related to wireless communications. Specific current

research topics include radiowave propagation, measurement and mobile time-varying channels modelling in vehicular applications, ultra-wideband (UWB) communication systems, MIMO systems and equalization techniques in digital wireless systems. Dr. Rubio was awarded by the Ericsson Mobile Communications Prize from the Spanish Telecommunications Engineer Association for his study on urban statistical radiochannels characterisation applied to wireless communications.



Gonzalo Llano R.

was born in Cali, Colombia. He received his M.S. degree in Technologies, Systems and Communications Networks from Technical University of Valencia (Spain) in 2007. He is currently a Ph.D. student and

researcher at the Radio and Wireless Communications Group (RWCG) in the iTEAM Research Institute at the Technical University of Valencia.

His research is focused on modeling and statistical characterization of UWB channels, adaptive modulation systems with multicarrier transmission for UWB (MB-OFDM UWB), security and quality of services in WPAN networks with UWB.



Juan Reig

was born in Alcoy, Spain, in 1969. He received the M.S. and Ph.D. degrees in Telecommunications Engineering from the Technical University of Valencia, Spain, in 1993 and 2000, respectively. He has been

a faculty member in the Department of Communications at the Technical University of Valencia, Spain since 1994, where he is now Associate Professor of Telecommunication Engineering. He is a member of the Radio and Wireless Communications Group (RWCG) of the Telecommunications and Multimedia Applications Research Institute (iTEAM). His areas of interest include fading theory, diversity, ultra-wide band systems and vehicular communications in V2V and V2I networks.